Journal of Chromatography A, 1236 (2012) 28–41

Contents lists available at SciVerse ScienceDirect

Journal of Chromatography A

journal homepage: www.elsevier.com/locate/chroma

Comparison of the fast gradient performance of new prototype silica monolithic columns and columns packed with fully porous and core–shell particles

Fabrice Gritti [a], Nobuo Tanaka [b], Georges Guiochon [a,*]

[a] Department of Chemistry, University of Tennessee, Knoxville, TN 37996-1600, USA
[b] GL Sciences, Inc., c/o Kyoto Monotech, 1095 Shuzei-cho, Kamigyo-ku, Kyoto 602-8155, Japan

ARTICLE INFO

Article history:
Received 6 December 2011
Received in revised form 14 February 2012
Accepted 16 February 2012
Available online 3 March 2012

Keywords:
Fast chromatography
Monolithic columns
Particulate columns
Gradient elution
Extra-column band broadening
Peak capacity

ABSTRACT

The gradient elution performance of narrow-bore 2.3 mm × 50 mm (N733) and wider bore 3.2 mm × 50 mm (N648 and N655) prototype silica monolithic columns was investigated and compared to the performance of commercially available columns packed with sub-2 μm fully porous particles (2.1 mm × 50 mm, 1.7 μm BEH-C_{18}, Waters) and sub-3 μm superficially porous particles (2.1 mm × 50 mm, 2.7 μm Halo-ES-Peptide-C_{18} (AMT), 1.7 and 2.6 μm Kinetex-C_{18}, Phenomenex). Results show that the two wide monolithic columns show peak capacities similar to the one measured for the Kinetex column. In contrast, the narrow-bore monolithic column delivers a lower performance (−30%) than the BEH, the Halo and the Kinetex columns. This work stresses out the importance of reducing the extra-column band broadening contribution of HPLC instruments when short 2.1 mm I.D. columns are used. The part of the instrument contribution originating downstream the column is important for all compounds; the one originating upstream the column is significant only for weakly retained compounds.

1. Introduction

The pharmaceutical and food industries are constantly challenging column manufacturers to prepare more permeable columns providing smaller height equivalent to a theoretical plate (HETP) [1]. For a given maximum column inlet pressure, more permeable columns are always preferred because they allow shorter analysis times and a significant gain in time. High column efficiencies are required to provide sufficiently high resolutions of the sample components, meaning that long columns are usually needed. This classical chromatographic *conandrum* between fast and high-resolution separations has successfully brought column technology toward the preparation and packing of smaller particles (down to 1.7 μm) along with the development of very high pressure liquid chromatographs [2]. Fast and efficient analyses could then be achieved with small volume 2.1 mm × 50 mm columns but at pressures routinely exceeding 400 bar [3]. In order to help coping with the problem of very high pressures, sub-3 μm shell particles emerged in 2006 [4–6]. Columns packed with these materials offer optimum plate heights comparable to those measured with columns packed with sub-2 μm fully porous particles but have twice to thrice larger column permeabilities [7–10], allowing their use with standard 400 bar instruments, provided that the contribution of the chromatograph to band broadening be minimized by replacing the standard parts with less voluminous ones [11].

The first generation of silica monolithic columns was introduced twelve years ago. These columns provided an exceptionally high permeability, close to that of columns packed with 10 μm particles [12]. Nevertheless, their minimum plate heights was also high, around 20 μm, so that 10 cm long columns could barely provide 5000 plates. In contrast, 5 cm long columns (2.1 and 3.0 mm I.D.) packed with sub-2 μm fully porous particles [13] and 10 cm long columns (4.6 mm I.D.) packed with sub-3 μm shell particles [7] are now able to produce about 15 000 and 30 000 plates, respectively. This difference in performance explains the limited success of the monolithic columns of the first generation. Their decline was soon attributed to large trans-column velocity biases [14], a direct consequence of their preparation process: the production of the rods involves an exothermic sol–gel reaction and is followed by a drying step [15] causing a shrinking of the rod and a large external porosity (70%). This velocity bias was confirmed by local electrochemical detection of the eluting band of a non-retained species at different radial positions across the outlet column diameter [16,17]. Relative velocity biases of about 3% and 5% were measured for 4.6 and 10 mm I.D. silica rods, respectively. Recently, manufacturers prepared more radially homogeneous silica structures [18]. Merck Millipore (Darmstadt, Germany) released last October a second generation of 4.6 mm × 100 mm silica monolithic columns. Recent investigations of their performance showed that these columns

* Corresponding author. Tel.: +1 865 974 0733; fax: +1 865 974 2667.
E-mail addresses: guiochon@ion.chem.utk.edu, guiochon@utk.edu (G. Guiochon).

0021-9673/$ – see front matter © 2012 Elsevier B.V. All rights reserved.
doi:10.1016/j.chroma.2012.02.046

Nomenclature

Roman letters

F_v	flow rate (m^3/s)
F_v	column phase ratio
G	intrinsic gradient steepness ($=S\Delta\varphi(t_0/t_G)$)
G	intrinsic gradient steepness of the last eluted compound ($=S_{last}\Delta\varphi(t_0/t_G)$)
G_{12}^2	gradient band compression factor
H	total column HETP (m)
$\overline{H}$	average column HETP experienced by the sample during gradient elution (m)
k	retention factor
k_i	retention factor of compound *i* in the RPLC checkout sample
k_0	retention factor extrapolated in pure water
K_0	specific permeability (m^2)
K_{Cell}	dispersion constant in Eq. (18)
K_{Inj}	dispersion constant in Eq. (21)
$k_{0,last}$	retention factor of the last retained compound extrapolated in pure water
k_F	apparent retention factor of the last eluted compound in gradient conditions
k_I	retention factor of the eluted compound when it enters the column
k_L	retention factor of the eluted compound when it exits the column
k_{last}	retention factor of the last eluted compound at the beginning of the gradient
l	capillary length (m)
L	column length (m)
P_c	theoretical peak capacity
$P_{c,exp}$	experimental peak capacity
r_c	capillary inner radius (m)
t	time variable (s)
t_D	dwell time (s)
t_0	column hold-up time (s)
t_9	gradient elution time of the last eluted compound of the RPLC checkout sample (s)
t_{last}	elution time of the last eluted compound in gradient conditions (s)
t_G	gradient time (s)
S	negative of the slope of the LSSM plot
S_{last}	LSSM slope parameter of the last eluted compound in gradient conditions
u_0	chromatographic linear velocity (m/s)
v_{Cell}	detection cell volume (m^3)
v_{Valve}	injection valve volume (m^3)
z	axial column coordinate (m)
$z_{catch,i}$	axial column coordinate at which the gradient is catching up with the compound *i* in the RPLC checkout sample (m)

Greek letters

ε_t	total porosity
ε_e	external porosity
ε_p	internal porosity
φ	volume fraction of acetonitrile in the mobile phase
φ_{start}	volume fraction of acetonitrile at the beginning of the gradient
φ_{end}	volume fraction of acetonitrile at the end of the gradient
φ_9	volume fraction of acetonitrile at which the last eluted compound of the RPLC checkout sample exits the column
$\Delta\varphi$	amplitude of the change in volume fraction during the gradient
Ψ	parameter defined in Eq. (7)
σ	peak standard deviation (s)
σ_t^2	total time variance (s^2)
$\sigma_{t,I}^2$	time variance associated with the band broadening taking place upstream the column (s^2)
$\sigma_{t,D}^2$	time variance associated with the band broadening taking place downstream the column (s^2)
$\sigma_{t,ex}^2$	extra-column time variance (s^2)
$\sigma_{t,Inj}^2$	time variance associated to the injected volume (s^2)
$\sigma_{t,seat}^2$	time variance associated with the band broadening taking place in the needle seat capillary (s^2)
$\sigma_{t,Viper}^2$	time variance associated with the band broadening taking place in the Viper connecting tube (s^2)
$\sigma_{t,Cell}^2$	time variance associated with the band broadening taking place in the detection cell (s^2)
$\sigma_{t,Connect}^2$	time variance associated with the band broadening taking place at the connections between the system parts (s^2)
ω	parameter defined in Eq. (6)
ω_9	baseline peak width of coumpound #9 in the RPLC checkout sample (s)
ρ	ratio of the solid core to the particle diameter for shell particles

have the efficiency of columns packed with 3.5 μm fully porous particles and the permeability of columns packed with 4.5 μm particles [19]. It was observed, however, that a small trans-column relative velocity bias subsists in these new columns (about to 1%). Kyoto Monotech (Kyoto, Japan) prepared prototype 3.2 mm × 50 mm silica monolithic columns that provide a performance equivalent to that of columns packed with 2 μm particles with the permeability of columns packed with 4 μm particles. Exceptionally, the minimum HETP of these latter columns was found to be smaller for non-retained analytes than for retained compounds in RPLC, demonstrating that this new silica structure combined with newly designed frits and endfittings generated monolithic columns having nearly no radial velocity biases.

The goal of this work is to assess the performance of the new prototype columns prepared by Kyoto Monotech (N731, N648, and N655) in gradient elution chromatography on a VHPLC instrument (1290 Infinity system from Agilent Technologies). Because the length of these columns is short (5 cm), they are well suited for fast analyses, if run at the maximum inlet pressure that these columns can withstand (~200 bar). Their peak capacity is compared to those of commercially available columns packed with sub-2 μm fully porous particles (1.7 μm BEH-C_{18}, Waters, Milford, USA) and sub-3 μm shell particles (1.7 and 2.6 μm Kinetex-C_{18}, Phenomenex, Torrance, USA) for the same analysis speed. Two test mixtures are used: the RPLC check out sample from Agilent Technologies (Little fall, DE, USA) and a home-made mixture of hydrocarbons produced by the green micro-algae *Botryococcus braunii* when incumbated under nitrogen stress conditions [20]. Theoretical expressions of the peak capacity (taking into account or not the peak compression during gradient elution) are used to extract an apparent isocratic HETP, *H*, assumed to be constant for all the components present in the mixture and for all mobile phase compositions. These *H* values permit a comparison of the relative performance of these new monolithic columns and of the best available particulate columns.

2. Theory

2.1. Peak capacity

The theory of gradient elution chromatography is well established [21,22]. The underlying theory required to assess the quality of a separation in gradient elution was developed [23] based on the definition of the peak capacity, P_c, which is defined as the upper limit of the number of resolvable components assuming a resolution of unity or:

$$P_c = 1 + \int_{t_0}^{t_{last}} \frac{1}{4\sigma} dt \quad (1)$$

where t_0 is the column hold-up time, t_{last} is the retention time of the last eluted peak, dt is a dummy time variable, and σ is the average time standard deviation of the peaks eluted during the gradient run.

During gradient elution, the rear part of the sample zone moves faster than its front part because the eluent strength increases constantly with passing time along the column. This phenomenon is better known under the name of band compression and can be theoretically calculated under certain conditions [24].

If we neglect band compression during the gradient run and assume that the local HETP, H, is the same for all mobile phase compositions and all compounds present in the sample mixture, the expression of the peak capacity is given by [23]:

$$P_c = 1 + \frac{1}{4}\sqrt{\frac{L}{H}}\frac{1}{G+1}\ln\left[\frac{G+1}{G}e^{Gk_F} - \frac{1}{G}\right] \quad (2)$$

where L is the column length, G is the intrinsic gradient factor, and k_F is the apparent retention factor of the last compound eluted during the gradient run. The gradient factor is written:

$$G = S\Delta\varphi\frac{t_0}{t_G} \quad (3)$$

where S is the slope of the relationship between the natural logarithm of the retention factor, k, measured under isocratic conditions and the organic solvent concentration, φ, in the case when the linear solvent strength (LSS) model ($\ln k = \ln k_0 - S\varphi$) applies, $\Delta\varphi$ is the change in solvent composition during the gradient, and t_G is the gradient run time.

Finally, the apparent retention factor, k_F, of the last eluted compound is related to the parameters G_{last}, S_{last} and $k_{0,last}$ through [23]:

$$k_F = \frac{1}{G_{last}}\ln[1 + G_{last}k_{last}] \quad (4)$$

where $k_{last} = k_{0,last}\exp(-S_{last}\varphi_{start})$ is the retention factor of this compound at the beginning of the gradient run and φ_{start} is the initial volume fraction of acetonitrile in water before the gradient starts.

With the same assumptions as made earlier for the derivation of Eq. (2), but taking into account the band compression factor in the expression of the peak width at column outlet, the peak capacity becomes [25]:

$$P_c = 1 + \frac{1}{4}\sqrt{\frac{3L}{\omega H}}\ln\left[\frac{2\omega e^{Gk_F} + G^2 - 6 + \psi}{G(2\sqrt{3\omega} + 3G + 6)}\right] \quad (5)$$

where

$$\omega = G^2 + 3G + 3 \quad (6)$$

$$\psi = 2\sqrt{\omega[(G^2-6)e^{Gk_F} + \omega e^{2Gk_F} + G^2 - 3G + 3]} \quad (7)$$

It is important to mention that both Eqs. (2) and (5) neglect the band broadening contributions of the HPLC instrument to the eluted peak width in gradient elution chromatography. They assume on-column injection at $z = 0$ and on-column detection at $z = L$. Obviously, and particularly for narrow-bore columns, band broadening taking place downstream the column (by dispersion in the connecting tubes and the detector cell) is not negligible at high flow rates [11,26]. Additionally, some band broadening takes place upstream the column (in the injection needle, the needle seat capillary, the injection valve, and the inlet capillary) and its contribution is significant for the peaks of the less retained compounds which are not compressed at the column inlet before the beginning of the gradient. This issue will be quantified in the next section based on the time variances. Finally, both Eqs. (2) and (5) assume that the dwell time of the HPLC system is strictly equal to zero. In fact, this is clearly unrealistic, in which case the less retained compounds of a complex mixture are eluted isocratically over a significant fraction of the column length before being caught by the gradient front.

2.2. Band broadening in gradient HPLC

The time variance, σ_t^2, of a compound measured after gradient elution is given by [11]:

$$\sigma_t^2 = \sigma_{t,I}^2\left[\frac{1+k_L}{1+k_I}\right]^2 + G_{12}^2\overline{H}L\left[\frac{1+k_L}{u_0}\right]^2 + \sigma_{t,D}^2 \quad (8)$$

where $\sigma_{t,I}^2$ is the time variance associated with the band broadening taking place between the injection needle and the column inlet ($z = 0$), k_L is the local retention factor of the sample when it reaches the column outlet ($z = L$), $k_I = k(\varphi_{start})$ is the retention factor of the sample when it enters the column, G_{12}^2 is the band compression factor (<1) [24,27–31], L is the column length, $\overline{H}$ is the average column plate height experienced by the sample during its gradient elution, u_0 is the chromatographic linear velocity (or L/t_0), and $\sigma_{t,D}^2$ is the time variance associated with the band broadening taking place between the column outlet and the detector cell (including volumetric and time related contributions). $\overline{H}$ is given by [27]:

$$\overline{H} = \frac{t_G}{t_0}\frac{1}{\Delta\varphi}\int_{\varphi_{start}}^{\varphi_{exit}}\frac{H(\varphi)}{k(\varphi)}d\varphi \quad (9)$$

where φ_{exit} is the mobile phase composition eluting a given compound at the column outlet, and $H(\varphi)$ and $k(\varphi)$ are the plate height and the retention factor of the compound at the mobile phase composition φ.

3. Experimental

3.1. Chemicals

The mobile phase was a mixture of acetonitrile and water. Both solvents were HPLC grade and were purchased from Fisher Scientific (Fair Lawn, NJ, USA). The RPLC checkout sample (1 mL) was purchased from Agilent Technologies (Little Fall, DE, USA). This mixture contains 100.3 μg/mL (±0.5%) of acetophenone, propiophenone, butyrophenone, valerophenone, hexanophenone, heptanophenone, octanophenone, benzophenone, and acetanilide dissolved in a water/acetonitrile (65/35, v/v) matrix. The homemade biological mixture containing hydrocarbons was produced by extraction with chloroform of a culture of the green alga *B. braunii showa* (race B), which was purchased from the University of Berkeley, CA, USA.

3.2. Apparatus

The 1290 Infinity HPLC system (Agilent Technologies, Waldbroen, Germany) liquid chromatograph used in this work includes a

Table 1
Columns used in this work: three prototypes silica-C_{18} monolithic columns prepared by Kyoto Monotech (N731, N648, and N655) and of three particulate columns (BEH-C_{18} and Kinetex-C_{18}) measured in our lab.

Column's name manufacturer	Column's serial number	Column's Dimension I.D. × length [mm] × [mm]	Total porosity[a]	Average mesopore size[b] [Å]
N648-C_{18} Kyoto Monotech	(Prototype)	3.2 × 50	0.722	65
N655-C_{18} Kyoto Monotech	(Prototype)	3.2 × 50	0.837	200
N733-C_{18} Kyoto Monotech	(Prototype)	2.3 × 50	0.857	145
1.7 μm BEH-C_{18} Waters	0197312581	2.1 × 50	0.573	115
1.7 μm Kinetex-C_{18} Phenomenex	573495-8	2.1 × 50	0.504	75
2.6 μm Kinetex-C_{18} Phenomenex	580765-98	2.1 × 50	0.506	75
2.7 μm Halo-ES-C_{18} AMT	USJA001257	3.0 × 50	0.521	125

[a]Value obtained from the corrected elution volume of uracil in a CH_3CN/H_2O (75/25, v/v) eluent mixture.
[b]Value estimated from the intersection of the exclusion and intrusion branches of the inverse size exclusion chromatography (ISEC) plots.

1290 Infinity Binary Pump with Solvent Selection Valves and a programmable auto-sampler. The injection volume is drawn into one end of the 20 μL injection loop. The reproducibility of the injection system is excellent as long as the sample volume drawn is larger than 0.2 μL. The instrument is equipped with a two-compartment oven and a multi-diode array UV–vis detection system. The system is controlled by the Chemstation software. The sample trajectory in the equipment involves the successive passage of its band through the series of:

- A 20 μL injection loop attached to the injection needle. The design of the injection system is such that the volume of sample drawn into the loop is the volume of sample injected into the column. This ensures an excellent injection repeatability.
- A small volume needle seat capillary (115 μm I.D., 100 mm long), ≃1.0 μL, located between the injection needle and the injection valve. The total volume of the grooves and connection ports in the valve is around 1.2 μL.
- Two 130 μm × 25 cm long Viper capillary tubes offered by the manufacturer (Dionex, Germering, Germany) were placed, one before, the second after the column. Each has a volume of 3.3 μL.
- A small volume detector cell, 0.8 μL, 10 mm path.

The dwell volume (e.g. the system volume from the mixing point of the two mobile phases coming from the high pressure pumps A and B to the column inlet) was measured at 125 μL (spring tube + 35 μL jet weaver V35 mixer + 254 μm × 50 cm green tubing) by running a sharp acetonitrile step (from pure water to 10% acetonitrile in volume) in absence of column. The detection wavelength was fixed at 195 nm.

It is important here to mention that the 130 μm × 25 cm Viper capillary tubes were preferred to any other connecting tubes (whether metallic or plastic) because they provide the smallest extra-column band broadening variance, the lowest pressure drops, and they could perfectly match (no connection voidage) to any column endfittings [32]. So, they allowed a fair comparison between the seven columns studied in this work since they are equipped with different types of column endfittings.

3.3. Columns

Three research monolithic columns were generously given by Kyoto Monotech (Kyoto, Japan), one 2.3 mm × 50 mm (N733) and two 3.2 mm × 50 mm (N648 and N655) columns. Two 2.1 mm × 50 mm columns packed with 1.7 and 2.6 μm shell Kinetex-C_{18} particles were generously offered by Phenomenex (Torrance, CA, USA). One 2.1 mm × 50 mm column packed with 1.7 μm BEH-C_{18} particles was kindly offered by Waters (Milford, MA, USA). The 3.0 mm × 50 mm column packed with 2.7 μm Halo-ES-Peptide-C_{18} shell particles was purchased from Advanced Material Technologies (Wilmington, DE, USA). Table 1 lists the total porosities, ε_t, and the average mesopore sizes of these seven columns after C_{18} derivatization and surface endcapping.

3.4. Gradient chromatography

In this work, we did not seek to achieve the maximum peak capacity per unit pressure or per unit time for each column tested. Instead, we compare the gradient performance of all the columns at constant gradient steepness (G) and constant analysis time (k_F). The unique gradient speed used was arbitrarily chosen so that the monolithic column was operated at the highest possible inlet pressure (maximum pressure drop: 200 bar). The unique gradient steepness was arbitrarily chosen according to the same following constraints, which represent the experimental conditions that will minimize the gradient analysis time of each column by fixing the gradient to about six times the column hold-up time.

For all columns, the same following gradient conditions were applied in order to spread the sample molecules over most of the gradient time window:

- First, we imposed that the retention factor, k_{last}, of the most retained compound in the sample mixture be 15 at the beginning of the gradient. The mobile phase composition, φ_{start}, at the start of the gradient is then given by:

$$k_{last}(\varphi_{start}) = 15 \tag{10}$$

- Second, we imposed that the retention factor, k_{last}, of the most retained compound in the sample mixture be 1 when the gradient ends. So, the mobile phase composition, φ_{end}, at the end of the gradient is given by:

$$k_{last}(\varphi_{end}) = 1 \tag{11}$$

- Finally, we imposed that the gradient elution time of the most retained compound in the sample mixture be one hold-up time unit shorter than the time needed for the gradient end to reach the column outlet. So, the gradient time, t_G, should be exactly given by the following relationship if the linear solvent strength model (LSSM) rigorously applies for this compound [23]:

$$t_G = t_0 + \frac{t_G}{S_{last}\Delta\varphi} \ln\left[1 + S_{last}\frac{\Delta\varphi}{t_G} k_{last}(\varphi_{start}) t_0\right] \tag{12}$$

where $k_{last}(\varphi_{start}) = 15$ and S_{last} (to be determined experimentally) is the best slope of the plot of the logarithm of the retention factor versus φ, assuming a linear solvent strength model (LSSM). t_0 is the hold-up time to be measured from the elution time of a non-retained compound (in this work, uracil).

A fair column-to-column gradient comparison requires that the same hold-up time, t_0, should be taken for all the seven columns tested. Therefore, the peak capacities and time peak widths could be directly compared for a constant analysis time. However, the

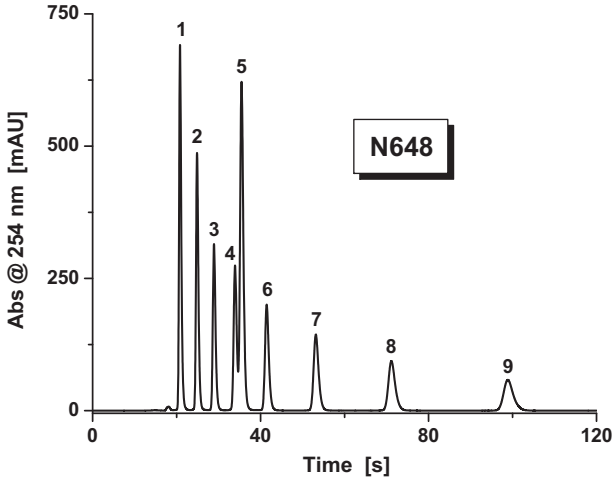

Fig. 1. Isocratic elution of the nine compounds contained in the RPLC checkout sample. Injection volume: 1 μL. Flow rate: 1 mL/min. Column: 3.2 mm × 50 mm N648 monolith. T = 297 K. Acetonitrile/water, 70/30 (v/v).

stationary phase structures being different, the average mesopore sizes and the surface chemistry are necessarily different from one column to the other and so are the S, φ_{start}, φ_{end}, and t_G gradient parameters. Therefore, the intrinsic gradient factor, G, cannot be rigorously kept constant for all columns. Nevertheless, as shown later, they are very close to each other.

4. Results and discussion

The first part of this work is devoted to the determination of the best LSSM parameters for all the components in the RPLC checkout sample and for the last most abundant compound in the biological extract of hydrocarbon molecules. From them, it is straightforward to determine the gradient parameters for a fair column-to-column comparison. The second part reports on the results of the gradient chromatography experiments performed at the fastest speed imposed by the pressure limitation of the silica monolithic columns (<200 bar).

4.1. Isocratic measurements

4.1.1. RPLC checkout samples

The RPLC checkout sample contains nine different low molecular weight compounds all at the concentration of 0.1 g/mL, including the least retained compound, acetanilide (peak #1), seven *n*-homologous compounds from acetophenone (peak #2) to propiophenone (peak #3), butyrophenone (peak #4), valerophenone (peak #6), hexanophenone (peak #7), heptanophenone (peak #8), octanophenone (peak #9), and benzophenone (peak #5), which elutes at a retention time slightly larger than that of propiophenone. Fig. 1 shows a chromatogram recorded under isocratic conditions (70% acetonitrile), performed with the 3.2 mm × 50 mm monolithic column N648. Benzophenone is easily recognizable in the chromatogram because its molar extinction coefficient at 254 nm is about twice that of its closest neighbor (propiophenone).

The retention factor of these nine analytes depends on two important column characteristics. The first is the phase ratio, $F = (1 - \varepsilon_t)/\varepsilon_t$, or ratio of the stationary phase to the bulk phase volume. It increases from 0.17 (N733) to 0.19 (N655), 0.39 (N648), 0.75 (BEH-C_{18}), 0.92 (Halo-ES-Peptide-C_{18} 2.7 μm), and 0.98 (Kinetex-C_{18} 1.7 and 2.6 μm). To provide comparable retention factors, columns with a small phase ratio usually require a mobile phase with a higher water content than those with a large phase ratio because their surface area is smaller. Because shell particles

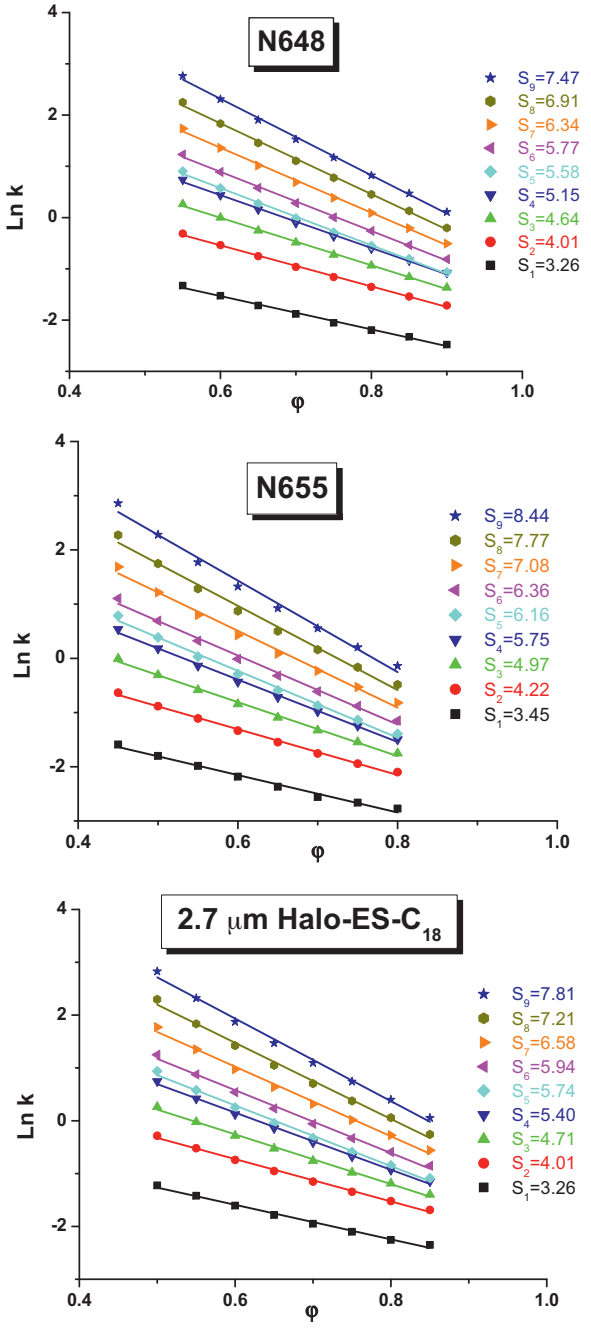

Fig. 2. Plots of the logarithm of the retention factors, ln k, of the nine compounds present in the RPLC checkout sample (see the names of the molecules in the text) as a function of the volume fraction, φ, of acetonitrile in the aqueous mobile phase. (Top) 3.2 mm × 50 mm N648 monolith, (middle) 3.2 mm × 50 mm N655 monolith, (bottom) 3.0 mm × 50 mm Halo-ES-Peptide-C_{18} column. T = 295 K, F_v = 1.0 mL/min.

contain a solid silica core, which does not contribute to retention, their actual phase ratio is $F = (1 - \varepsilon_e)(1 - \rho^3)(1 - \varepsilon_p)/\varepsilon_t$, where ε_e is the external porosity (~0.4 [7–10]), ρ is the ratio of the core to the particle diameter (~0.6 for Halo and 0.7 for Kinetex [8]), and ε_p is the shell porosity (~0.3). So, the actual phase ratios of the Kinetex and Halo columns are likely to be around 0.5–0.6 instead of 0.9–1.0 when counting the solid non-porous core as an active part of the stationary phase. The second column characteristic is the mesopore size. Because retention is directly related to the accessible surface area, the smaller this size, the larger the specific surface area of the bed and the larger the retention factors. In this work, the average mesopore sizes are 65 (N648), 75 (Kinetex-C_{18} 1.7 and 2.6 μm),

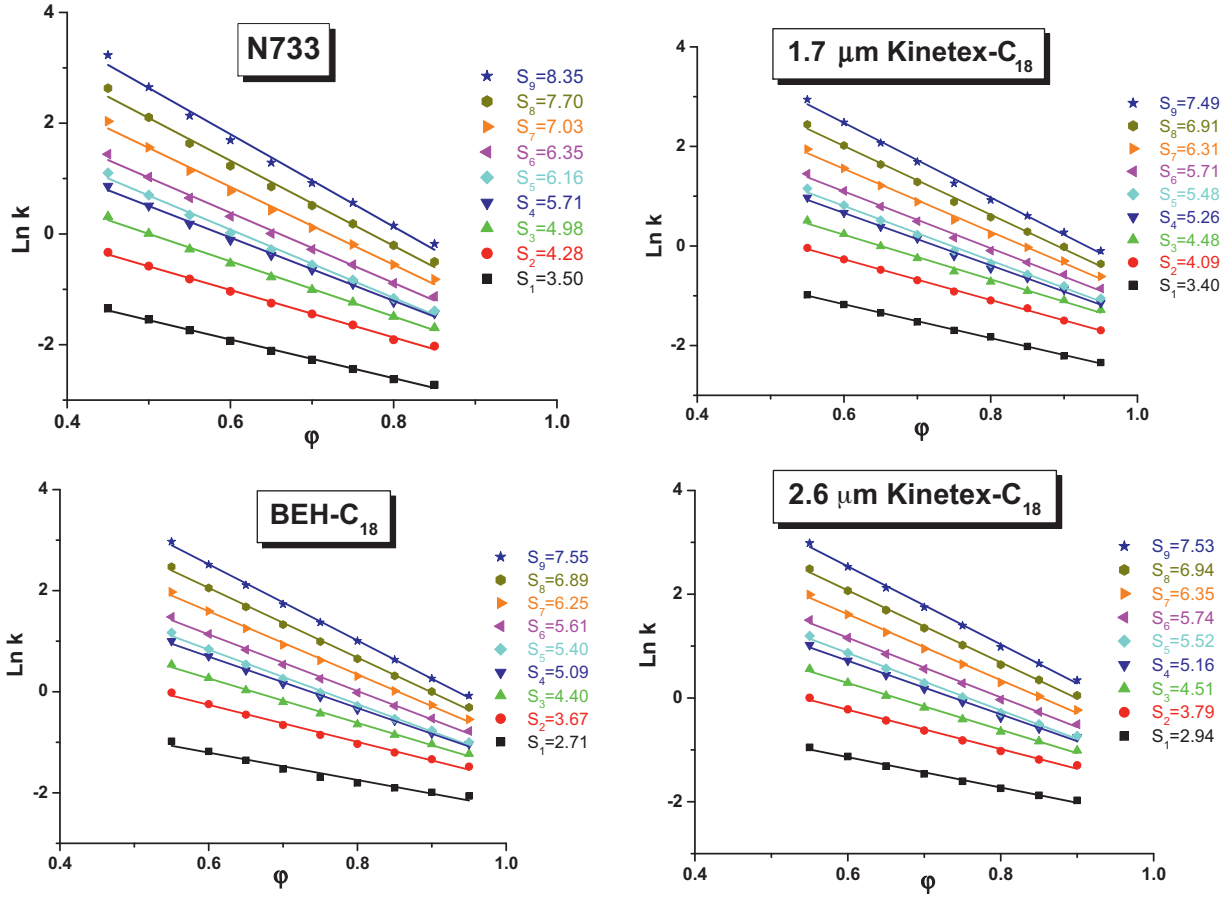

Fig. 3. Plots of the logarithm of the retention factors, ln k, of the nine compounds present in the RPLC checkout sample (see the names of the molecules in the text) as a function of the volume fraction, φ, of acetonitrile in the aqueous mobile phase. (Top left) 2.3 mm × 50 mm N733 monolith, (bottom left) 2.1 mm × 50 mm BEH-C_{18} columns, (top right) 2.1 mm × 50 mm 1.7 μm Kinetex-C_{18} column, and (bottom right) 2.1 mm × 50 mm 2.6 μm Kinetex-C_{18} column. T = 295 K. F_v = 0.4 mL/min.

115 (BEH-C_{18}), 130 (Halo-ES-Peptide-C_{18}), 145 (N733), and 200 Å (N655).

For reasons explained above, the plots of the logarithm of the retention factors versus the volume fraction of acetonitrile must be carefully measured for the seven columns tested. This step is critical for performing a fair comparison between the separations in gradient elution obtained with columns having different physicochemical properties. Figs. 2 and 3 show these plots for the nine compounds present in the RPLC checkout sample. They confirm that the less retentive columns are the monolithic columns since their phase ratio are low ($0.17 < F < 0.39$). As expected, the silica rods with the largest average mesopore sizes (N655: 200 Å, N733: 145 Å) are the less two retentive columns. The largest retention factors are measured with the packed columns due to their large phase ratios ($0.50 < F < 0.75$) and their relatively small average mesopore sizes (75, 115, and 125 Å). Remarkably, the monolithic column N648 is as retentive as the packed columns due to its relatively large phase ratio (0.4 versus 0.2) and small mesopore size (65 Å, only).

Fig. 4 shows the dependence of the LSSM parameter, S, of the columns on the number, N, of carbon atoms in the alkyl chain in the homologous n-alkanophenones: ($2 < N < 8$). Strikingly, the columns can be sorted into three categories: the monoliths N655 and N733 (the less retentive stationary phases, with the largest values of S), Kinetex 1.7 and 2.6 μm, BEH, and N648 (the most retentive columns with the lowest values of S), and Halo (in an intermediate category). The smaller the retention, the larger the parameter S, and the steeper the slope, $\Delta S/\Delta N$, of the increment of S per increment of N. These ratios increase from 0.59 (N648) to 0.60 (Kinetex 1.7 μm), 0.61 (Kinetex 2.6 μm), 0.63 (BEH), 0.64 (Halo), 0.68 (N733), and 0.70 (N655). Accordingly, in order to fulfill the conditions Eqs. (10) and (11), we must use slightly different eluent compositions during the gradient elution on the monilithic columns N655 or N733 and on the monolithic column N648 and the packed columns.

Based on the LSSM parameters of the most retained compound octanophenone (ln $k_{0,last}$ and S_{last}), it is now possible to set the volume fractions of acetonitrile at the beginning (φ_{start}) and at the end

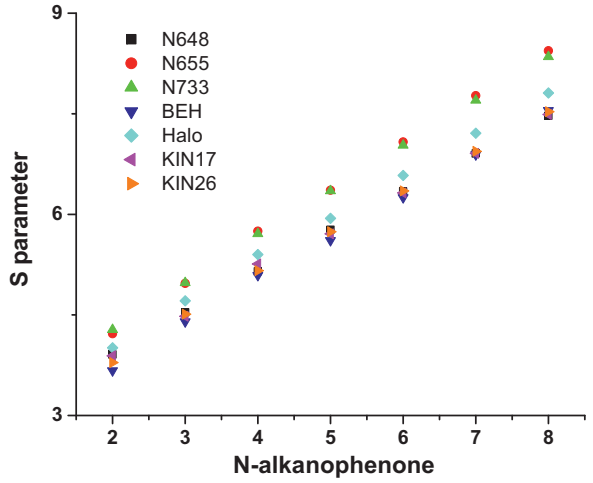

Fig. 4. Plots of the best S parameter of the LSSM versus the number of carbon, N, in the homologous series of N-alkanophenones for the seven stationary phases studied in this work. Note the linear increase of S with increasing N.

Table 2
Gradient HPLC conditions applied for the analysis of the Agilent RPLC checkout sample (9 compounds). They include the starting and ending mobile phase compositions, φ_{start} and φ_{end}, respectively, the flow rate, F_v, the gradient time, t_G, the intrinsic gradient factor, G, and the inlet column pressure before the gradient starts, P_{inlet}, for all seven columns tested in this work. Note that the hold-up time, t_0, was kept constant for all columns.

Column's name manufacturer	Column's dimension I.D. × length [mm] × [mm]	φ_{start}	φ_{end}	F_v [mL/min]	t_0 [min]	t_G [min]	G	P_{inlet} [bar]
N648-C_{18} Kyoto Monotech	3.2 × 50	0.556	0.916	2.50	0.116	0.603	0.378	212
N655-C_{18} Kyoto Monotech	3.2 × 50	0.462	0.779	2.90	0.116	0.606	0.365	232
2.7 μm Halo-ES-peptide-C_{18} AMT	3.0 × 50	0.510	0.862	1.59	0.116	0.590	0.389	300
N733-C_{18} Kyoto Monotech	2.3 × 50	0.496	0.826	1.53	0.116	0.592	0.389	169
1.7 μm BEH-C_{18} Waters	2.1 × 50	0.580	0.940	0.86	0.116	0.598	0.369	605
1.7 μm Kinetex-C_{18} Phenomenex	2.1 × 50	0.576	0.940	0.75	0.116	0.595	0.389	454
2.6 μm Kinetex-C_{18} Phenomenex	2.1 × 50	0.581	0.953	0.75	0.116	0.584	0.401	258

(φ_{end}) of the linear gradient so that the retention factors of this compound are fixed at 15.0 and 1.0, respectively. Table 2 lists these volume fractions (third and fourth columns) for the seven columns tested in this work. These values could not have been guessed a priori before performing these isocratic measurements.

4.1.2. Application to the analysis of the nonpolar extract of an alga culture

The analysis of a hydrocarbon mixture extracted from the micro-alga *B. braunii* was recently investigated with a series of 4.6 mm × 100 mm Kinetex-C_{18} columns [20] in gradient elution with acetonitrile and water with an initial volume fraction of acetonitrile of 70%. Fig. 5 shows the isocratic run performed with the monolithic column N648 at a flow rate of 2 mL/min (70% acetonitrile). Fig. 6 gathers the plots of the logarithm of the retention factor, ln k, of the last eluted compound as a function of the volume fraction of acetonitrile, φ. Consistent with the plots given in Fig. 4, they confirm that the monolithic columns N655 and N733 are the less retentive stationary phases (due to their small phase ratio and large average mesopore size). The BEH, Kinetex, and N648 columns remain the most retentive ones (due to their large phase ratio and/or small average mesopore size) while the Halo column conserves an intermediate retention strength. The negative of the best slopes, S, are equal to 9.75 (N648), 9.45 (N655), 9.35 (Halo), 9.32 (N733), 9.72 (BEH), 9.74 (Kinetex 1.7 μm), and 9.62 (Kinetex 2.6 μm). The largest S parameter measured for the RPLC checkout sample was about 7.5 for the Kinetex columns. Therefore, the hydrophobicity of the last retained compound in the extract sample is equivalent to that of undecano or dodecanophenone (17–18 carbon atoms, 26–28 hydrogen atoms, one oxygen atom, or a molecular weight around 250–260 g/mol).

Because the retention factor measured for the Kinetex 2.6 μm column and pure acetonitrile is close to 1.3, we imposed that the retention factor at the end of the gradient be 1.3 (instead of 1.0 for the RPLC checkout sample). The retention factor of the most retained analyte was kept at 15. Table 3 lists the corresponding starting (φ_{start}) and ending (φ_{end}) volume fractions of acetonitrile applied during the gradient elution runs of the seven columns.

4.2. Fast gradient chromatography

4.2.1. RPLC checkout samples

All the gradient experimental parameters are listed in Table 2. They were determined according to the constraints Eqs. (10)–(12), for a fixed hold-up time t_0 = 0.116 min. This hold-up time was not chosen randomly but it corresponds to the highest possible mobile phase velocity possible with the less permeable monolithic columns, N648 ($K_0 = 1.35 \times 10^{-14}$ m^2) and N655 ($K_0 = 1.65 \times 10^{-14}$ m^2) [32]. The corresponding inlet pressures recorded were 212 bar (F_v = 2.50 mL/min, φ_{start} = 0.553) and 232 bar (F_v = 2.90 mL/min, φ_{start} = 0.462), respectively. These high inlet pressures were still considered safe because the pressure drop

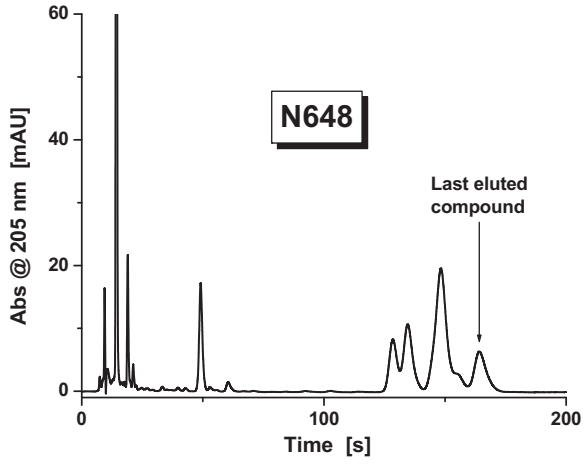

Fig. 5. Isocratic elution of the components of the extract of a culture of the micro-alga *Botryococcus braunii*. Injection volume: 1 μL. Flow rate: 2 mL/min. Column: 3.2 mm × 50 mm N648 monolith. T = 297 K. Acetonitrile/water, 70/30 (v/v). 1 μL injection.

recorded in the absence of the column, at 3 mL/min, were about 50 bar (depending on the initial mobile phase composition, typically around 50% acetonitrile in volume). Therefore, the actual pressure at the column inlet remains slightly smaller than 200 bar, as recommended by the manufacturer. As expected, based on the calculation of the gradient conditions for each column, the intrinsic

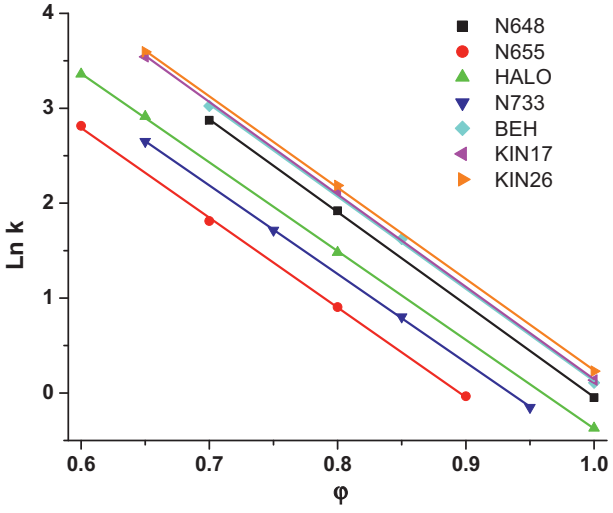

Fig. 6. Plots of the logarithm of the retention factors, ln k, of the last eluted compounds found in the extract of the micro-alga culture *Botryococcus braunii* as a function of the volume fraction, φ, of acetonitrile in the aqueous mobile phase. The seven columns indicated in the legend, were used.

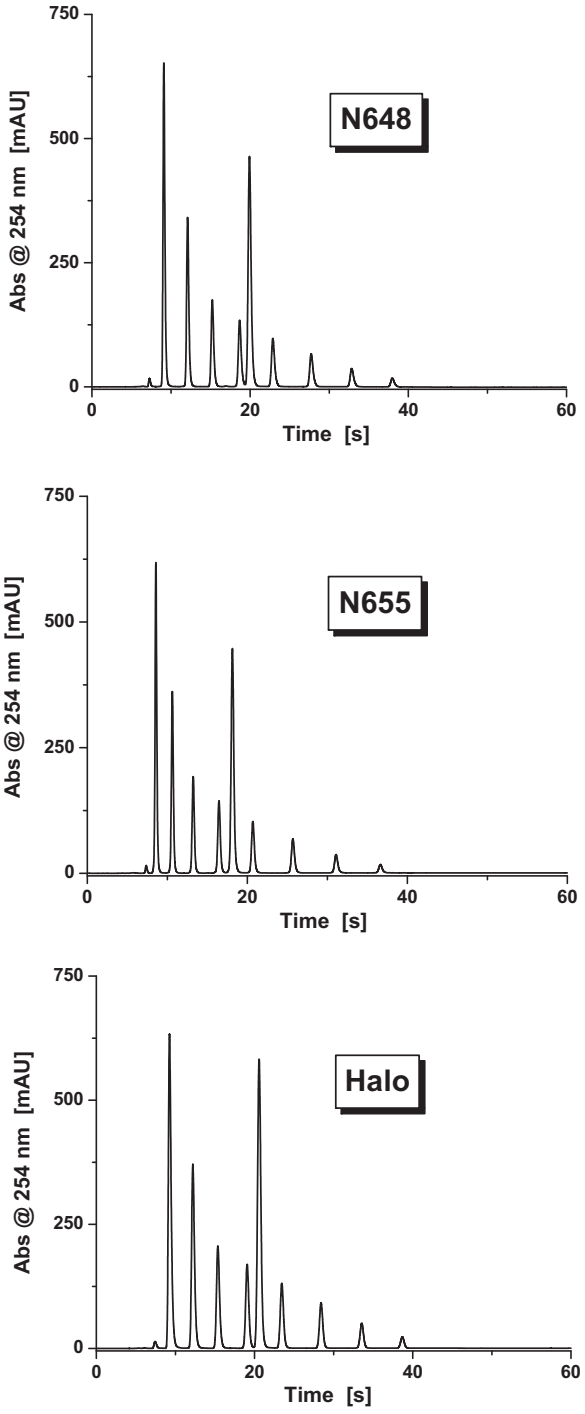

Fig. 7. Gradient elution chromatograms of the RPLC checkout sample. The hold-up time was fixed at $t_0 = 0.116$ min. $T = 297$ K. See experimental conditions in Table 2. (Top) 3.2 mm × 50 mm N648 monolith, (middle) 3.2 mm × 50 mm N655 monolith, (bottom) 3.0 mm × 50 mm Halo-ES-Peptide-C_{18} column.

gradient factors, G, given by Eq. (3) (see the one but last column in Table 2), are nearly equal for all the columns ($0.383 \pm 3.4\%$ standard deviation). The comparison between the gradient performance of the seven columns is now possible. Note that the volume of the injected sample was proportional to the cross-section area of the column, e.g., 1 μL (3.2 mm I.D. N648 and N655), 0.9 μL (3.0 mm I.D. Halo), 0.5 μL (2.3 mm I.D. N733), and 0.4 μL (2.1 mm I.D. BEH, Kinetex 1.7 and 2.6 μm).

The seven gradient chromatograms are shown in Figs. 7 and 8. For all the columns, the hold-up time was 7.0 seconds (0.116 min × 60 s/min). The dwell volumes were the same, at 0.125 mL. Therefore, the dwell time, t_D, or time necessary for the gradient to reach the column inlet depends on the flow rate applied. According to the flow rates listed in Table 2 (fifth column), these dwell times are to 3.0 (N648), 2.6 (N655), 4.7 (Halo), 4.9 (N733), 8.0 (BEH), and 10.0 seconds (Kinetex 1.7 and 2.6 μm). This explains why the elution time of the last eluted compound, octanophenone (peak #9), varies slightly from one column to the next. For instance, the gradient actually starts (10.0–4.9) = 5.1 s later for the Kinetex columns than for the monolith N733 column, in agreement with the difference between the retention times of octanophenone (∼44 s on Kinetex versus 39 s on N733).

The retention factors, $k_1(\varphi_{start})$ on the different columns of the first eluted compound (peak # 1, acetanilide) before the gradient reaches the column inlet are 0.25 (N648), 0.19 (N655), 0.27 (Halo), 0.22 (N733), 0.33 (BEH), 0.34 (Kinetex 1.7 μm and 2.6 μ). Eventually, the gradient catches up with acetanilide (the time origin is when the injection valve actuates and the mixing starts in the pump) if [27]:

$$t_D < k_1(\varphi_{start}) t_0 \tag{13}$$

According to this inequality, the dwell times should be smaller than 1.8 (N648), 1.3 (N655), 1.9 (Halo), 1.5 (N733), 2.3 (BEH), and 2.4 seconds (Kinetex 1.7 and 2.6 μm). In practice, the dwell times are all larger than 2.6 seconds as above mentioned. Therefore, the first component acetanilide is eluted isocratically along all the columns. Similarly, the initial retention factors, $k_2(\varphi_{start})$, of the second eluted compound (peak #2, acetophenone) are 0.71 (N648), 0.49 (N655), 0.70 (Halo), 0.60 (N733), 0.85 (BEH), and 0.85 (Kinetex 1.7 μm and 2.6 μm). The critical dwell times for this compound are thus 5.0 (N648), 3.4 (N655), 4.9 (Halo), 4.2 (N733), 6.0 (BEH), and 6.0 seconds (Kinetex 1.7 and 2.6 μm). They are barely smaller than the actual dwell times for the N648, N655, and Halo columns, which are run fast (at 2.5, 2.9, and 1.59 mL/min), but they are still larger than those for N733, BEH, and both Kinetex columns, which are run more slowly (at 1.53, 0.86, and 0.75 mL/min, only). So, this compound is fully or mostly eluted isocratically. It is only for the third eluted compound (propiophenone) that the gradient actually catches up with the peak before it reaches the column outlet. None of the migration distances is negligible compared to the column length ($L = 5$ cm), since they are 1.7 (N648), 2.1 (N655), 2.8 (Halo), 3.3 (N733), 4.0 (BEH), and 4.9 cm (Kinetex 1.7 and 2.6 μm). This result is important because it shows that the mixture component i injected in the sample is eluted first isocratically, up to the distance $z_{catch,i}$, which is a simple function of the column length, the hold-up time, the initial retention factor, and the dwell time [27]:

$$z_{catch,i} = \frac{L}{t_0} \frac{t_D}{k_i(\varphi_{start})} \tag{14}$$

Beyond that critical distance, the compound peak speeds up according to the fundamental relationship of the gradient theory. Therefore, in order to compare precisely the peak capacities of the different columns tested in this work, it is important to focus on the time band width of the most retained peak (peak #9, octanophenone), which is eluted along the column mostly under gradient conditions. Indeed, for all columns, $k_9(\varphi_{start})$ is as large as 15 and $z_{catch,9}$ is much smaller than the column length (5 cm), at 0.14 (N648), 0.12 (N655), 0.22 (Halo), 0.23 (N733), 0.38 (BEH), and 0.48 cm (Kinetex 1.7 and 2.6 μm). The theoretical peak capacity in Eqs. (2) and (5) represent then a good estimate of the column performance (under the assumptions detailed in the theory section) and one can then estimate the apparently constant HETP, H, of each column from the experimental peak width of octanophenone. In other words, as a first approximation, we assume that the gradient peak widths of the compounds eluted during the gradient between t_0 and t_{last} are the same. Table 4 lists the experimental baseline

Table 3
Gradient HPLC conditions applied for the analysis of the extract sample produced by the micro-algae *Botryococcus braunii*. They include the starting and ending mobile phase compositions, φ_{start} and φ_{end}, respectively, the flow rate, F_v, the gradient time, t_G, the intrinsic gradient factor, G, and the inlet column pressure before the gradient starts, P_{inlet}, for all seven columns tested in this work. Note that the hold-up time, t_0, was kept constant for all columns.

Column's name manufacturer	φ_{start}	φ_{end}	t_G [min]	G	P_{inlet} [bar]
N648-C_{18} Kyoto Monotech	0.718	0.970	0.657	0.437	180
N655-C_{18} Kyoto Monotech	0.609	0.866	0.657	0.427	212
2.7 μm Halo-ES-peptide-C_{18} AMT	0.670	0.932	0.655	0.433	269
N733-C_{18} Kyoto Monotech	0.644	0.906	0.661	0.431	146
1.7 μm BEH-C_{18} Waters	0.734	0.986	0.664	0.433	504
1.7 μm Kinetex-C_{18} Phenomenex	0.737	0.988	0.661	0.432	368
2.6 μm Kinetex-C_{18} Phenomenex	0.743	0.998	0.661	0.434	203

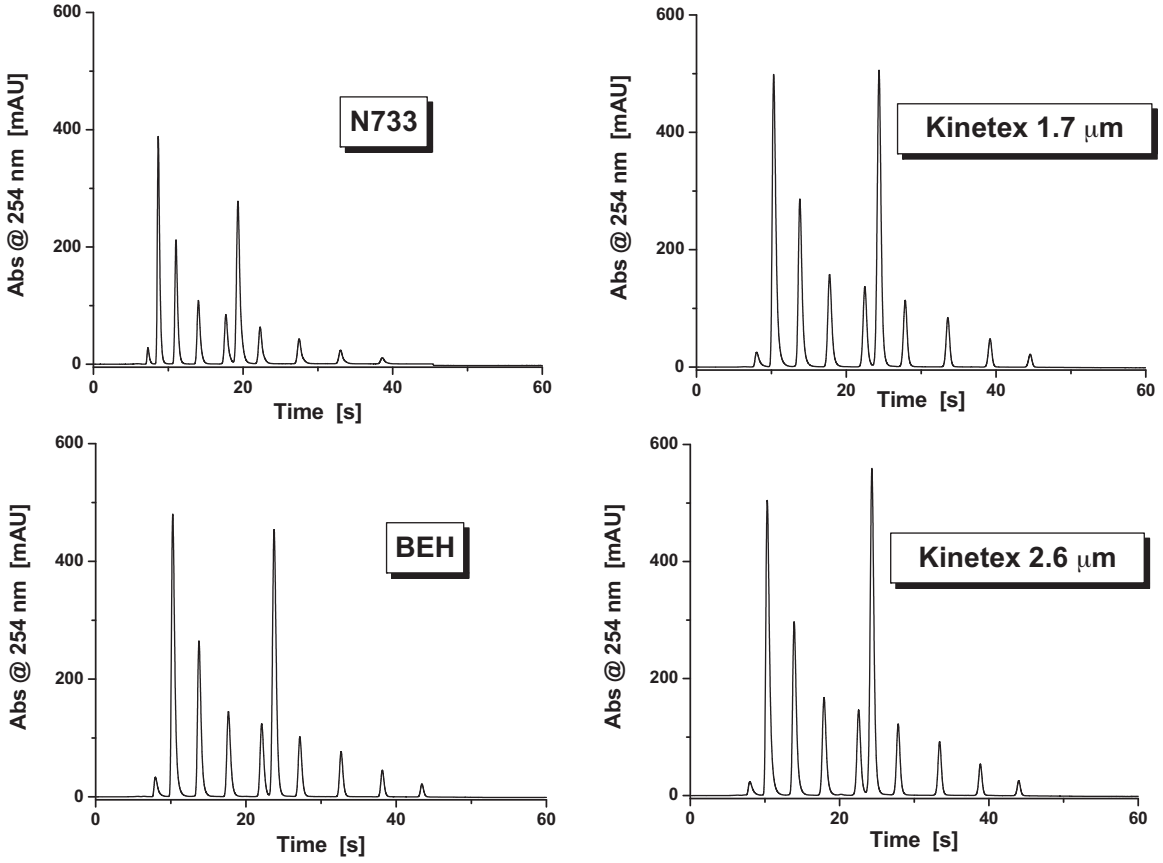

Fig. 8. Gradient elution chromatograms of the RPLC checkout sample. The hold-up time was fixed at $t_0 = 0.116$ min. $T = 297$ K. See experimental conditions in Table 2. (Top left) 2.3 mm × 50 mm N733 monolith, (bottom left) 2.1 mm × 50 mm BEH-C_{18} columns, (top right) 2.1 mm × 50 mm 1.7 μm Kinetex-C_{18} column, and (bottom right) 2.1 mm × 50 mm 2.6 μm Kinetex-C_{18} column.

Table 4
Experimental elution time of octanophenone (t_9), baseline peak width of octanophenone (ω_9), sum of the hold-up and dwell times ($t_0 + t_D$), peak capacities ($P_{c,exp}$), and apparent column HETP (H).

Column's name manufacturer	t_9 [s]	$t_0 + t_D$ [s]	Baseline peak width, ω_9 [s]	Peak capacity, $P_{c,exp}$ [a]	Effective plate height, H [b] [μm]
N648-C_{18} Kyoto Monotech	37.98	10.00	1.04	27.90	18.8
N655-C_{18} Kyoto Monotech	36.64	9.59	1.01	27.78	19.1
2.7 μm Halo-ES-C_{18} AMT	38.69	11.72	0.99	28.24	18.0
N733-C_{18} Kyoto Monotech	38.63	11.90	1.34	20.93	33.8
N731-C_{18} Kyoto Monotech	38.61	11.90	1.46	19.29	40.0
1.7 μm BEH-C_{18} Waters	43.43	15.77	0.95	30.11	15.9
1.7 μm Kinetex-C_{18} Phenomenex	44.56	17.00	1.05	27.25	19.5
2.6 μm Kinetex-C_{18} Phenomenex	44.00	17.00	0.98	28.55	17.3

[a] Values measured from Eq. (15).
[b] Apparent values calculated from Eq. (2).

peak widths, ω_9, of octanophenone and the peak capacities, $P_{c,exp}$ measured by:

$$P_{c,exp} = 1 + \frac{t_9 - t_0 - t_D}{\omega_9} \quad (15)$$

These experimental peak capacities are in the range between 27 and 30 for all the columns, except that measured for the small I.D. monolithic column, N733, which performs less well, with a peak capacity of only 21. To check the repeatability of these results, we performed the same gradient but with the column N731 (same dimensions and same gel composition [32]). Again, the experimental peak capacity was found low, at 19, showing that the result was not due to a column failure. Furthermore, columns N731 and N733 are the most permeable ones and the inlet pressure was below 200 bar (~170 bar). Fig. 8 shows that the peak of octanophenone is clearly tailing on column N733 (and its height is relatively small), whereas peaks are more symmetrical on the other columns.

Assuming the absence of extra-column band broadening ($\sigma_{t,I} = \sigma_{t,D} = 0$) and peak compression ($G_{12} = 0$), Eq. (2) directly applies. On the one hand, the constant HETP, H, can be extracted for each column. These values are listed in the last column of Table 4. On the other hand, the true HETPs of octanophenone, measured in a weak eluent ($14 < k < 20$), are listed in the fifth row of Table 5. It is striking that the HETPs determined from Eq. (2) are twice to thrice larger than the true HETPs of octanophenone measured under strongly retained conditions. Therefore, the extra-column parts (injection needle, 1.0 μL needle seat capillary, 1.2 μL injection valve, 2 × 3.3 μL Viper connecting tubes, and 0.8 μL UV detection cell) and their connections must contribute to the broadening of the peaks observed in gradient elution. The time variance contribution, $\sigma^2_{t,ex}$, of these system parts to the total band broadening of octanophenone in gradient elution is given by Eq. (16) [11,31]:

$$\sigma^2_{t,ex} = \sigma^2_{t,I}\left[\frac{1 + k_9(\varphi_9)}{16}\right]^2 + \sigma^2_{t,D} \quad (16)$$

In this equation, $k_9(\varphi_9)$ is the retention factor of octanophenone when it exits from the column. The factor 16 is the term $1 + k_9(\varphi_{start})$ with $k_9(\varphi_{start}) = 15$ according to the first constraint imposed in this work. Assuming piston flow displacement for the acetonitrile gradient, the composition of the mobile phase, φ_9, associated with the elution of octanophenone at the column outlet and at time t_9 (second column in Table 4) is given by [27]:

$$t_9 = t_0 + \frac{16}{15}t_D + \frac{\varphi_9 - \varphi_{start}}{\varphi_{end} - \varphi_{start}}t_G \quad (17)$$

According to Eq. (17) and the experimental values for t_9, the values of φ_9 listed in Table 6 (third column) are 0.832 (N648), 0.696 (N655), 0.775 (Halo), 0.741 (N733), 0.852 (BEH), 0.850 (Kinetex 1.7 μm), and 0.861 (Kinetex 2.6 μm). Assuming the best LSSM (see solid lines in Figs. 2 and 3), the corresponding retention factors, k_9, of octanophenone at the column outlet are then 1.8 (N648), 1.8 (N655), 1.7 (Halo), 1.8 (N733), 1.9 (BEH), 1.8 (Kinetex 1.7 μm), and 1.8 (Kinetex 2.6 μm). In other words, the variance contributions of the injection needle, the needle seat capillary, the injection valve, and the inlet capillary, $\sim 0.03 \times \sigma^2_{t,I}$, to the total extra-column time variance in gradient elution chromatography, $\sigma^2_{t,ex}$, are most likely negligible compared to the additional peak variance of octanophenone due to broadening taking place downstream the column, $\sigma^2_{t,D}$. Yet, an accurate estimate of both $\sigma^2_{t,I}$ and $\sigma^2_{t,D}$ is needed in order to obtain a definitive measurement of $\sigma^2_{t,ex}$ in Eq. (16).

It is not possible to directly measure the sole contribution of the outlet Viper connecting tube and of the detection cell, $\sigma^2_{t,D}$. Only the total extra-column peak variance can be measured, by replacing the column with a ZDV union connector. These total time variances were measured at the applied gradient flow rates of 2.50 (N648, 1.0 μL injected, $\varphi_9 = 0.832$), 2.90 (N655, 1.0 μL injected, $\varphi_9 = 0.696$), 1.59 (Halo, 0.9 μL injected, $\varphi_9 = 0.775$), 1.53 (N733, 0.5 μL injected, $\varphi_9 = 0.741$), 0.86 (BEH, 0.4 μL injected, $\varphi_9 = 0.852$), 0.75 (Kinetex 1.7 μm, 0.4 μL injected, $\varphi_9 = 0.850$) and 0.75 mL/min (2.6 μm, 0.4 μL injected, $\varphi_9 = 0.862$). The results are given in the fifth column of Table 6. The relevant problem consists in estimating the contributions of the sole UV detection cell and outlet Viper capillary or $\sigma^2_{t,D}$ to the total extra-column variance measured. This can only be done by estimating semi-empirically the variance contributions of each system part. Recently, an investigation of the minimization of the band broadening contributions of the Agilent 1290 Infinity system [33] showed that the UV cell contribution depends on the flow rate applied, giving [33]:

$$\sigma^2_{t,Cell} = \frac{V^2_{Cell}}{K_{Cell}(F_v)F_v^2} \quad (18)$$

Assuming an ideal plug flow along the 320 μm × 10 mm detection cell, K_{Cell} should be equal to 12. However, dispersion in this channel is due to the parabolic flow profile and, at flow rates of 0.04, 0.40, and 4.0 mL/min, K_{Cell} was found to be equal to 5.5, 2.5, 0.5, respectively. From a parabolic interpolation, one can reasonably interpolate K_{Cell} to values of 1.75, 1.60, 1.10, 1.05, 0.75, and 0.65 at the gradient flow rates of 0.75, 0.86, 1.53, 1.59, 2.5, and 2.9 mL/min, respectively, applied during the gradient elution runs.

Similarly, the injected plug of the sample is not the expected ideal rectangular profile. Its time variance was given by [33]:

$$\sigma^2_{t,Inj} = \frac{V^2_{Inj}}{K_{Inj}(F_v)F_v^2} \quad (19)$$

Again, the constant K_{Inj} would be equal to 12 if the injection needle could deliver an ideal rectangular injection plug. However, for flow rates between 0.4 and 4.0 mL/min, a constant excess of 6 μL^2 was measured compared to the peak variance expected for an ideal injection when the injection volume increased from 4 to 20 μL (+32 μL^2). Therefore, K_{Inj} is estimated at 10.

The time variances, $\sigma^2_{t,Viper}$ and $\sigma^2_{t,Seat}$, through the 130 μm × 250 mm cylindrical Viper connecting tube and the 115 μm × 100 mm needle seat capillary are estimated from a simplified coupling theory of band dispersion in cylindrical tubes [34]:

$$\sigma^2_{t,Viper} = \frac{\pi^2 r_c^4 l^2}{F_v(3F_v + 24\pi l D_m)} \quad (20)$$

where $r_c = 65$ μm is the capillary inner radius, $l = 250$ mm is the capillary length, and $D_m = 8.7 \times 10^{-6}$ cm^2/s is the bulk diffusion coefficient of octanophenone (molar volume at its boiling point of 270 cm^3/mol) estimated from the Wilke and Chang correlation [35] at 297 K, in an acetonitrile/water eluent mixture (75/25, v/v, viscosity 0.58 cP).

The injection valve is considered as a simple mixer volume and the time variance is written:

$$\sigma^2_{t,Valve} = \frac{V^2_{Valve}}{F_v^2} \quad (21)$$

Finally, the contribution, $\sigma^2_{t,Connect}$, to the extra-column peak variance of all the system connections is obtained from the following subtraction:

$$\sigma^2_{t,Connect} = \sigma^2_{t,ex} - \sigma^2_{t,Inj} - \sigma^2_{t,Seat} - \sigma^2_{t,Valve} - 2\sigma^2_{t,Viper} - \sigma^2_{t,Cell} \quad (22)$$

There are four connections upstream the column (injection needle/needle seat capillary, needle seat capillary/injection valve, injection valve/inlet Viper tube, and inlet Viper tube/column) but only two (inlet Viper tube/column and inlet Viper tube/detection

Table 5
Experimental plate heights, H, measured for the last eluted compound, octanophenone, in strongly retained conditions.

	N648-C_{18} Kyoto Monotech	N655-C_{18} Kyoto Monotech	2.7 μm Halo-ES-C_{18} AMT	N733-C_{18} Kyoto Monotech	1.7 μm BEH-C_{18} Waters	1.7 μm Kinetex-C_{18} Phenomenex	2.6 μm Kinetex-C_{18} Phenomenex
F_v [mL/min]	1.0	1.0	1.0	0.5	0.4	0.4	0.4
Aceonitrile/water (v/v)	55/45	45/55	50/50	50/50	55/45	55/45	55/45
k	15.9	17.4	16.9	14.2	19.7	19.0	19.8
H [μm]	8.0	11.0	6.0	20.2	5.7	5.5	5.5

Table 6
Mobile phase composition (φ_9) when the last eluted compound, octaphenone, exits the column, total extra-column time variances ($\sigma^2_{t,ex}$) measured in absence of column, experimental gradient total peak variance (σ^2_t) of octanophenone, average gradient plate height ($G^2_{12}\overline{H}$), and the sole column variance ($\sigma^2_{t,column}$).

Column's name Manufacturer	F_v	φ_9	V_{Inj}	$\sigma^2_{t,ex}$ [s^2]	σ^2_t [s^2]	Plate height, $G^2_{12}\overline{H}$ [μm][a]	$\sigma^2_{t,column}$ [s^2]
N648-C_{18} Kyoto Monotech	2.50	0.832	1.0	0.0053	0.0597	7.4	0.0569
N655-C_{18} Kyoto Monotech	2.90	0.696	1.0	0.0046	0.0634	7.9	0.0610
2.7 μm Halo-ES-C_{18} AMT	1.59	0.775	0.9	0.0131	0.0471	5.7	0.0407
N733-C_{18} Kyoto Monotech	1.53	0.741	0.5	0.0124	0.0957	11.6	0.0891
1.7 μm BEH-C_{18} Waters	0.86	0.852	0.4	0.0384	0.0458	3.3	0.0271
1.7 μm Kinetex-C_{18} Phenomenex	0.75	0.850	0.4	0.0502	0.0509	3.5	0.0271
2.6 μm Kinetex-C_{18} Phenomenex	0.75	0.862	0.4	0.0501	0.0511	3.6	0.0274

[a] Values obtained by solving Eq. (2).

cell) downstream the column. Therefore, the following expressions for $\sigma^2_{t,I}$ and $\sigma^2_{t,D}$ are proposed:

$$\sigma^2_{t,I} = \sigma^2_{t,Inj} + \sigma^2_{t,Seat} + \sigma^2_{t,Valve} + \sigma^2_{t,Viper} + \frac{2}{3}\sigma^2_{t,Connect} \quad (23)$$

and

$$\sigma^2_{t,D} = \sigma^2_{t,Viper} + \sigma^2_{t,Cell} + \frac{1}{3}\sigma^2_{t,Connect} \quad (24)$$

All these individual extra-column peak variances ($\sigma^2_{t,I}$, $\sigma^2_{t,D}$, $\sigma^2_{t,Inj}$, $\sigma^2_{t,Seat}$, $\sigma^2_{t,Valve}$, $\sigma^2_{t,Viper}$, $\sigma^2_{t,Cell}$, and $\sigma^2_{t,Connect}$) are listed in Table 7. This table shows that the contribution of the injection volume, which is small in gradient experiments, is always negligible. Similarly, despite the large applied flow rates, the injection valve does not generate any significant band broadening. In the second position in terms of relative importance to their contributions to band broadening, the needle seat capillary and the detection cell account for about 4 and 7% of the total extra-column peak width. The six connections account for about 22% and the two Viper capillary tubes for as much as 70% of total band broadening along the channels of the HPLC system.

The contributions $\sigma^2_{t,I}$ and $\sigma^2_{t,D}$ being known semi-empirically, one can estimate the effective average gradient HETP, $G^2_{12}\overline{H}$, for the different columns tested in this work by solving numerically Eq. (16). These plate heights, listed in the seventh column in Table 6, are 7.4 (N648), 7.9 (N655), 5.7 (Halo), 11.6 (N733), 3.3 (BEH), 3.5 (Kinetex 1.7 μm), and 3.6 μm (Kinetex 2.6 μm). They show the actual performance of all these columns, free from the extra-column band broadening contributions, when analysts impose a column hold-up time as short as 7 seconds, an inlet retention factor of 15.0, and an outlet retention factor of 1.8. Clearly, under such conditions, the packed columns generate smaller column HETPs than the monolithic columns. Nevertheless, the performance of these packed columns are not much better than those of the monolithic columns N648 and N655, due to the extra-column contributions, which account for 5% (N648), 4% (N655), 14% (Halo), 7% (N733), 41% (BEH), 47% (Kinetex 1.7 μm), and 46% (Kinetex 2.6 μm) of the total gradient time variance. Therefore, although it is an excellent, modern instrument, the 1290 Infinity HPLC system tends to level the performance of the two types of columns. The new silica monolithic columns provide the same experimental peak capacities as the packed columns. Except for the monolith N733, the apparent gradient performance of all the columns tested here appears to be nearly equivalent.

The relatively poor performance of the monolithic columns can be explained easily: they do not operate under optimal conditions in fast gradient chromatography, whereas the packed columns do. There are two reasons for that [32]:

- The flow rates imposed to the columns N648 (2.5 mL/min, u_S = 5.2 mm/s), N655 (2.9 mL/min, u_S = 6.0 mm/s), and N733 (1.53 mL/min, u_S = 6.1 mm/s) are significantly larger than their optimal superficial velocity of 1.5–2.0 mm/s at which the minimum HETP (5–6 μm) of the moderately retained naphthalene was measured [32]. The actual HETPs of naphthalene at these high superficial linear velocities were 7.5 μm (N648), 7.0 μm (N655), and 8.5 μm (N733). In contrast, the minimum HETP is often observed at reduced interstitial velocities as large as 10–15

Table 7
Time peak variance contributions of the different parts of the 1290 Infinity System to the total extra-column time variance. The flow rate applied to each column are listed in Table 5.

Column's name manufacturer	$\sigma^2_{t,I}$ [s^2]	$\sigma^2_{t,D}$ [s^2]	$\sigma^2_{t,Inj}$ [s^2]	$\sigma^2_{t,Seat}$ [s^2]	$\sigma^2_{t,Valve}$ [s^2]	$\sigma^2_{t,Viper}$ [s^2]	$\sigma^2_{t,Cell}$ [s^2]	$\sigma^2_{t,Connect}$ [s^2]
N648-C_{18} Kyoto Monotech	0.0027	0.0027	<0.00005	0.0002	<0.00005	0.0019	0.0005	0.0009
N655-C_{18} Kyoto Monotech	0.0023	0.0023	<0.00005	0.0001	<0.00005	0.0014	0.0004	0.0012
2.7μm Halo-ES-C_{18} AMT	0.0069	0.0062	<0.00005	0.0005	<0.00005	0.0043	0.0009	0.0031
N733-C_{18} Kyoto Monotech	0.0062	0.0061	<0.00005	0.0005	<0.00005	0.0046	0.0009	0.0017
1.7 μm BEH-C_{18} Waters	0.0205	0.0180	<0.00005	0.0015	0.0001	0.0131	0.0020	0.0087
1.7 μm Kinetex-C_{18} Phenomenex	0.0271	0.0230	<0.00005	0.0020	0.0001	0.0163	0.0023	0.0131
2.6 μm Kinetex-C_{18} Phenomenex	0.0271	0.0229	<0.00005	0.0020	0.0001	0.0163	0.0023	0.0130

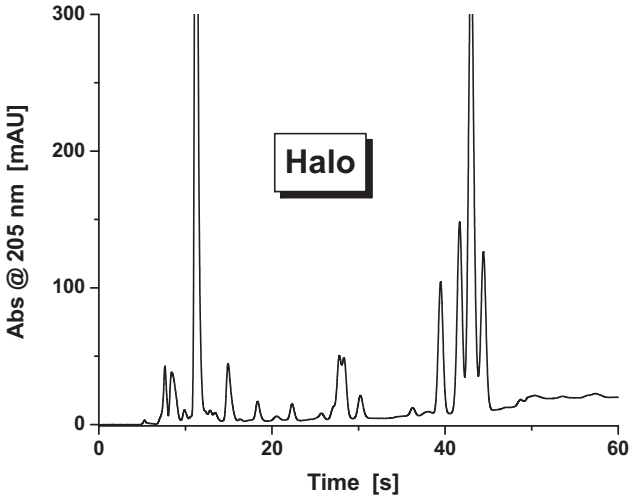

Fig. 9. Gradient elution chromatograms of the non-polar extract of the culture of the micro-algae *Botryococcus braunii*. The hold-up time was fixed at $t_0 = 0.116$ min. $T = 297$ K. See experiemntal conditions in Table 7. (Top) 3.2 mm × 50 mm N648 monolith, (middle) 3.2 mm × 50 mm N655 monolith, (bottom) 3.0 mm × 50 mm Halo-ES-Peptide-C_{18} column.

for columns packed with shell particles [36,37] and 5–10 for sub-2 μm fully porous particles [13]. In this work, the interstitial reduced linear velocities of octanophenone were $\nu = 29$ (Halo), 20 (BEH), 18 (Kinetex 1.7 μm), and 27 (Kinetex 2.6 μm). Therefore, the short narrow-bore columns packed with Halo, BEH, Kinetex 1.7 μm, and Kinetex 2.6 μm particles show a small increase above their optimal HETPs (1.7 × 2.7 = 4.6 μm [38], 2 × 1.7 = 3.4 μm [13], 2.0 × 1.7 = 3.4 μm, and 1.5 × 2.6 = 3.9 μm [38], respectively). Actually, the fast gradient conditions applied in this work favor the packed columns because their HETP curves are nearly flat at high reduced velocities.

- The optimum HETP (~4 μm) of these new prototype monolithic columns was observed for poorly retained species [32]. However, the results in Table 5 demonstrate that this no longer applies to strongly retained compounds like the last eluted compounds in the analyses done here. HETP as high as 8.0 μm (N648), 11.0 μm (N655), and 20.2 μm (N733) were actually measured for retention factors in the range $14 < k < 20$. In contrast, packed columns always show better performance for retained than for non-retained analytes because trans-column velocity biases are more efficiently relaxed due to a larger residence time in the column and a faster diffusivity through the particles [39,40]. To this regard, again, standard gradient conditions are definitely more favorable for commercial packed than for these prototype monolithic columns.

4.2.2. Application to the analysis of the nonpolar extract of an alga culture

An earlier investigation by gradient analysis of this extract showed that its most retained compounds have about 20–25 carbon atoms and a molecular weight around 300 g/mol [20]. The gradient elution runs were performed at a constant velocity for all columns, the same as that applied for the gradient analysis of the RPLC checkout sample ($t_0 = 7$ s). Fig. 9 (large I.D. columns) and 10 (small I.D. columns) show the chromatograms of the extract mixture produced by a culture of the alga *B. braunii*. It is difficult to

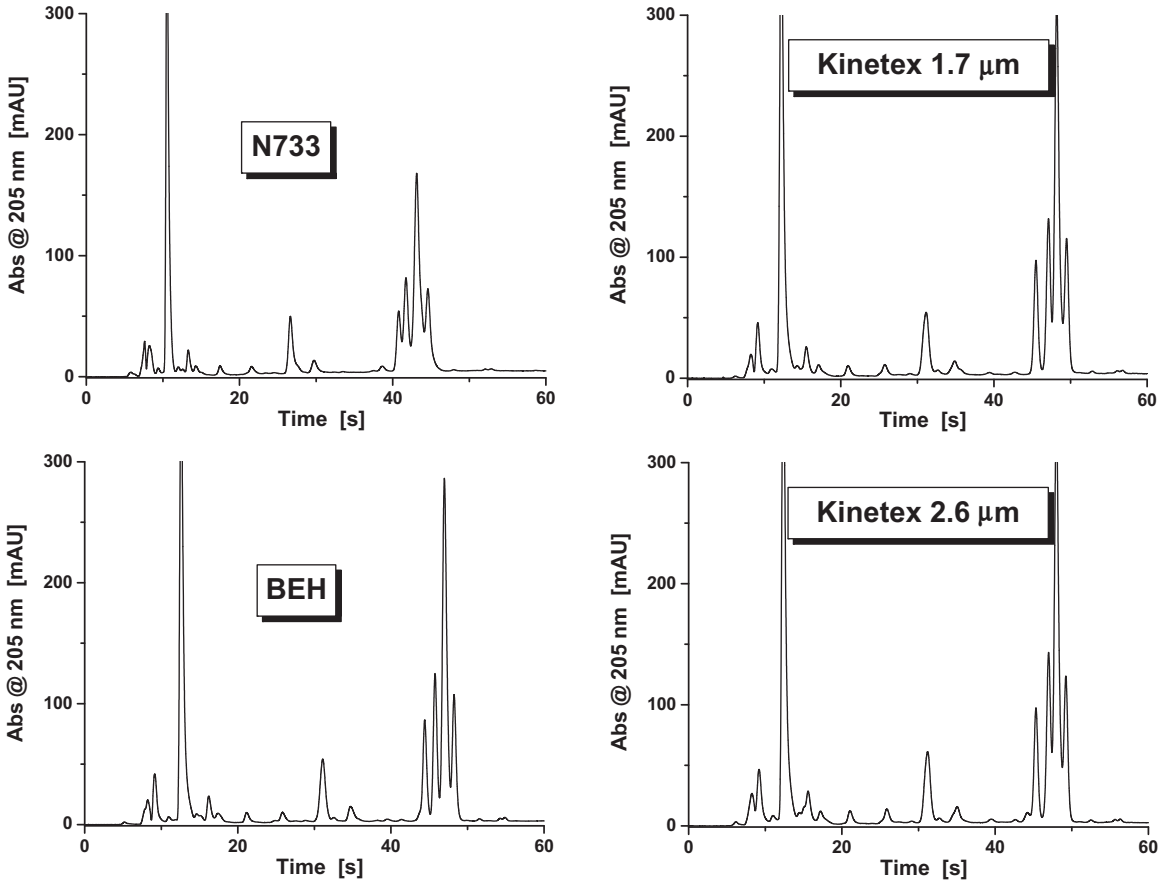

Fig. 10. Gradient elution chromatograms of the non-polar extract of the culture of the micro-algae *Botryococcus braunii*. The hold-up time was fixed at $t_0 = 0.116$ min. $T = 297$ K. See experimental conditions in Table 7. (Top left) 2.3 mm × 50 mm N733 monolith, (bottom left) 2.1 mm × 50 mm BEH-C_{18} columns, (top right) 2.1 mm × 50 mm 1.7 μm Kinetex-C_{18} column, and (bottom right) 2.1 mm × 50 mm 2.6 μm Kinetex-C_{18} column.

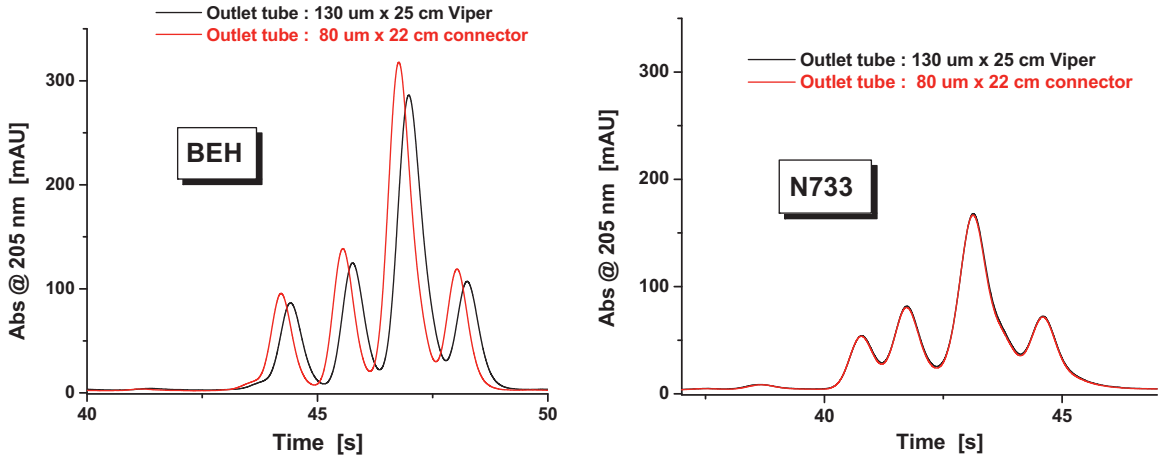

Fig. 11. Effect of the reduction of the volume of the outlet capillary on the resolution of the last four abundant compounds in the non-polar extract of the culture of the micro-algae *Botryococcus braunii*. (Left) 2.1 mm × 50 mm BEH-C_{18} columns and (right) 2.3 mm × 50 mm N733 monolithic column. The gradient conditions are given in Table 7. Note the quasi undistinguishable chromatograms for the monolithic column and the improvement of the separation with the BEH column.

make a quantitative estimate of the peak capacity of these analyses because the separations of the most abundant components and of lesser abundant ones is poor. All the peaks appear to be asymmetrical, which renders inaccurate and poorly precise any measurement of the peak capacity. Yet, the relative column performance can be assessed from the peak shape of the last four eluted compounds. The best resolutions of these four compounds are visibly obtained with the packed columns. Once again, the monolithic column N733 performs less well than the other two monolithic columns (N648 and N655), which confirm the previous observations based on the analysis of the RPLC check out sample.

Remarkably, although the intrinsic apparent gradient plate heights, $G_{12}^2\overline{H}$, of the packed columns (3.3, 3.5, 3.6, and 5.7 μm) are definitely smaller than those of the monolithic columns (7.4, 7.9, and 11.6 μm), the differences in peak widths and peak heights are not obvious in Figs. 9 and Fig. 10, except for the monolith N733. In theory, 2.3 and 2.1 mm packed columns should show better performance than the monolithic column N733 if the extra-column peak variance due to diffusion in the outlet Viper tube was reduced. This is demonstrated in Fig. 11, which compares the resolution power of the last four most abundant compounds before and after replacing the outlet 130 μm × 25 cm Viper tube (3.3 μL) with a 80 μm × 22 cm metallic tube (1.1 μL, only). There is in the left graph (BEH column, intrinsic apparent plate height of 3.3 μm) a net increase of the peak height with a better peak resolution whereas, in the right graph (N733 column, intrinsic apparent plate height of 11.6 μm), the two chromatograms are nearly undistinguishable. In conclusion, in spite of considerable progress over the first generation of monolithic columns, the new narrow-bore monolithic columns tested in this work appears to still perform less well than the commercial packed columns in fast gradient chromatography. In practice, however, when operated with a standard VHPLC instrument, they provide comparable performance in gradient separations.

5. Conclusion

The separation performance of three new 2.3 mm × 50 mm (N733) and 3.2 mm × 50 mm (N648 and N655) prototype silica monolith columns were compared in fast gradient elution chromatography to those of commercial packed columns of the same length and similar inner diameter (3.0 mm × 50 mm 2.7 μm shell Halo, 2.1 mm × 50 mm 1.7 μm fully porous BEH, 2.1 mm × 50 mm 1.7 μm and 2.6 μm shell Kinetex) for the same speed t_0. The same instrument, experimental conditions, and samples were used for this purpose. The shortest hold-up time, t_0, achievable with the monolithic columns with acetonitrile/water (50/50, v/v) mobile phase, at room temperature was about seven seconds (the largest allowed inlet pressure of 200 bar was reached under such conditions). It was kept the same for all columns. Because these columns have completely different stationary phase structures and surface chemistries, the gradient analyses were performed at constant initial and final retention factors for the last eluted component of the sample. This ensures that the intrinsic gradient factors are the same for all columns. Finally, the gradient measurements were made with an optimized VHPLC instrument, equipped with a small volume injection valve (1.2 μL), needle seat capillary (1.0 μL), and detection cell (0.8 μL). In order to make a fair comparison between the columns, universal 130 μm × 250 mm inlet and outlet Viper connectors (3.3 μL each) were used between the instrument and the columns. This removes any suspicion of a possible existence of different and nefarious void volumes between standard metallic/plastic endfittings and the seven different column inlet/outlet endfittings.

The apparent performance of the wide 3.2 mm I.D. monolithic columns (N648 and N648) proved to be nearly equivalent (−3%) to that of the Halo column. Noteworthy, the contribution of the column to the overall band broadening observed in gradient elution is about 95% for the monolithic columns and only 85% for the Halo column, which provides a smaller apparent HETP (5.7 μm) than the monolithic columns (7.4 and 7.9 μm, respectively) in excellent agreement with their performance measured under isocratic conditions, identical to those at the beginning of the gradient. In contrast, the performance of the narrow-bore 2.3 mm I.D. monolithic column (N733) are inferior (by −30%) to those of the commercial 2.1 mm I.D. BEH and Kinetex columns, despite the fact that the variance of the peaks eluted from these columns accounts for only 50% of the total peak variance measured for these commercial packed columns versus 93% for the monolithic column. This finding is consistent with the large isocratic HETP measured at the beginning of the gradients for the monolithic column and the apparent column HETP derived from the peak variance recorded in gradient elution. These last HETPs were 11.6 μm for the monolithic column N733 but only 3.3 (BEH), 3.5 (Kinetex 1.7 μm), and 3.6 μm (Kinetex 2.6 μm).

In conclusion, the new prototype silica monolithic columns do not seem to be designed to operate at their best in fast gradient elution for two main reasons: (1) they do not generate HETPs for strongly retained compounds that are as small as those observed for non-retained compounds (≃4 μm). Obviously, in gradient elution chromatography, at least 50% of the sample components are

strongly retained. In this work, for instance, the retention factor of the last eluted compound decreases from 15 to 1.8 during its migration along the column; (2) the superficial velocities imposed to the monolithic columns to run such fast gradients are twice to thrice larger than their optimum velocities. Consequently, they deliver larger HETPs than the optimum values of 5 μm measured for moderately retained analytes ($k \sim 2$) under isocratic conditions.

From a more general point of view, this work emphasizes the critical need to minimize the extra-column band broadening contributions that originate downstream the column for early eluters, particularly for small volume columns (such as the 2.1 mm × 50 mm ones that are becoming popular) when they deliver plate heights smaller than 5 μm. Obviously, the band broadening contributions that originate upstream the column are much less of an issue, as long as the ratio of the retention factor of the compound at the column inlet to that at the column outlet is sufficiently large. This is obviously not the case for the early eluted compounds. Finally, in fast gradient chromatography, a small dwell volume is required in order to minimize the fraction of the column length along which compounds run isocratically before the gradient catches up with them.

Acknowledgements

This work was supported in part by the cooperative agreement between the University of Tennessee and the Oak Ridge National Laboratory. We thank Tivadar Farkas (Phenomenex, Torrance, CA, USA) and Martin Gilar (Waters, Milford, MA, USA) for the generous gifts of the Kinetex-C_{18} and BEH-C_{18} columns, respectively. We also thank Marie-Agnes Perdu for the preparation of the biological sample extracted from the micro-algae *B. braunii*.

References

[1] 37th International Symposium on High Performance Liquid Phase Separations and Related Techniques, Dalian, China, October 8–11, 2011.
[2] J.R. Mazzeo, U.D. Neue, M. Kele, R.S. Plumb, Anal. Chem. 77 (2005) 460A.
[3] 32nd International Symposium on High Performance Liquid Phase Separations and Related Techniques, Baltimore, MD, May 10–16, 2008.
[4] J.J. Kirkland, T.J. Langlois, J.J. DeStefano, Am. Lab. 39 (2007) 18.
[5] J.J. DeStefano, T.J. Langlois, J.J. Kirkland, J. Chromatogr. Sci. 46 (2008) 254.
[6] F. Gritti, G. Guiochon, J. Chromatogr. A 1157 (2007) 289.
[7] F. Gritti, I. Leonardis, D. Shock, P. Stevenson, A. Shalliker, G. Guiochon, J. Chromatogr. A 1217 (2010) 1589.
[8] F. Gritti, I. Leonardis, J. Abia, G. Guiochon, J. Chromatogr. A 1217 (2010) 3219.
[9] F. Gritti, G. Guiochon, J. Chromatogr. A, in preparation.
[10] F. Gritti, G. Guiochon, J. Chromatogr. A, in preparation.
[11] F. Gritti, C. Sanchez, T. Farkas, G. Guiochon, J. Chromatogr. A 1217 (2010) 3000.
[12] M. Kele, G. Guiochon, J. Chromatogr. A 960 (2002) 19.
[13] F. Gritti, G. Guiochon, J. Chromatogr. A 1217 (2010) 1485.
[14] G. Guiochon, J. Chromatogr. A 1168 (2007) 101.
[15] H. Minakuchi, K. Nakanishi, N. Soga, N. Ishizuka, N. Tanaka, Anal. Chem. 68 (1996) 3498.
[16] K.S. Mriziq, J.A. Abia, Y. Lee, G. Guiochon, J. Chromatogr. A 1193 (2008) 97.
[17] J. Abia, K. Mriziq, G. Guiochon, J. Chromatogr. A 1216 (2009) 3185.
[18] K. Hormann, T. Mullner, S. Bruns, A. Holtzel, U. Tallarek, J. Chromatogr. A 1222 (2012) 46.
[19] F. Gritti, G. Guiochon, J. Chromatogr. A 1225 (2012) 79.
[20] F. Gritti, M.-A. Perdu, G. Guiochon, J. Chromatogr. A 1229 (2012) 148.
[21] P. Jandera, J. Churacek, Gradient Elution in Column Liquid Chromatography – Theory and Practice, Elsevier, Amsterdam, 1985.
[22] L. Snyder, High Performance Liquid Chromatography – Advances and Perspectives, Elsevier, Amsterdam, 1986.
[23] U. Neue, J. Chromatogr. A 1079 (2005) 153.
[24] H. Poppe, J. Paanakker, J. Bronckhorst, J. Chromatogr. 204 (1981) 77.
[25] F. Gritti, G. Guiochon, J. Chromatogr. A 1217 (2010) 1604.
[26] F. Gritti, G. Guiochon, J. Chromatogr. A 1217 (2010) 7677.
[27] F. Gritti, G. Guiochon, J. Chromatogr. A 1145 (2007) 67.
[28] F. Gritti, G. Guiochon, J. Chromatogr. A 1178 (2008) 79.
[29] F. Gritti, G. Guiochon, J. Chromatogr. A 1212 (2008) 35.
[30] F. Gritti, G. Guiochon, J. Chromatogr. A 1215 (2008) 64.
[31] F. Gritti, G. Guiochon, J. Chromatogr. A 1216 (2009) 6124.
[32] F. Gritti, G. Guiochon, J. Chromatogr. A 1227 (2012) 82.
[33] F. Gritti, G. Guiochon, J. Chromatogr. A 1218 (2011) 4632.
[34] K.J. Fountain, U.D. Neue, E.S. Grumbach, D.M. Diehl, J. Chromatogr. A 1216 (2010) 5979.
[35] C. Wilke, P. Chang, AIChE J. 1 (1955) 264.
[36] F. Gritti, G. Guiochon, J. Chromatogr. A 1217 (2010) 5069.
[37] F. Gritti, G. Guiochon, Chem. Eng. Sci. 65 (2010) 6310.
[38] F. Gritti, G. Guiochon, J. Chromatogr. A 1218 (2011) 1592.
[39] F. Gritti, G. Guiochon, J. Chromatogr. A 1217 (2010) 6350.
[40] F. Gritti, G. Guiochon, J. Chromatogr. A 1221 (2012) 2.